KWARTALNIK ELEKTRONIKI I TELEKOMUNIKACJI, 2003, 49, z. 3, ss. 271-294

Efficient Tolerance Analysis of Continuous-Time G_m-C Filters

SŁAWOMIR KOZIEŁ

Faculty of Electronics, Telecommunications and Informatics,
Gdańsk, University of Technology 80-952 Gdańsk, Poland
e-mail: koziel@ue.eti.pg.gda.pl.

Otrzymano 2002.10.02
Autoryzowano 2002.11.25

In the paper, an efficient approach to tolerance analysis of arbitrary G_m-C filters is investigated. We present a general structure of G_m-C filter of arbitrary order as well as its matrix description. Using this approach, we derive formulas that allow us to calculate the change of filter transfer function caused by the deviation of filter element values from their nominal values. At the expense of some approximations we are able, with these formulas, to determine transfer function deviation with low computational cost, which makes them suitable to perform statistical analysis of arbitrary G_m-C filters. It can also be used to analyse the influence of parasitics on filter characteristics. Several application examples including Worst Case analysis of high-order G_m-C filters are presented and discussed.

Keywords: G_m-C filters, tolerance analysis, statistical analysis.

1. INTRODUCTION

Recently an increasing interest in the design of continuous-time (CT) filters based on the transconductance-capacitor (G_m-C) technique has been observed [1], [2]. The transconductors and operational transconductance amplifiers (OTAs) offer a higher bandwidth than their voltage-mode counterparts, i.e., voltage operational amplifiers. Due to this, high frequency integrated filters are mostly realised as the G_m-C ones [9]. In this approach the basic building block is a simple CT integrator for which the key performance parameter is the phase shift at its unity-gain frequency [3]-[15]. Moreover, transconductance elements can be easily tuned electronically [6], [7] and have a better suitability for operating in reduced supply environment.

In the synthesis of G_m-C filters one wants to achieve several different objectives. The most important goal is, of course, that the filter structure should realise the desired transfer

function $H(s)$. Moreover, the filter should contain a small number of components, since it results in reduction of noise, parasitic effects and power consumption. The structures containing only grounded capacitors are also more attractive, because grounded capacitors can absorb parasitic capacitances and need smaller chip areas than floating ones [2]. Eventually, we want filter structures which have large dynamic range and low sensitivity.

It is important for filter design purposes to develop efficient tools for performing statistical analysis of G_m-C filters. Monte Carlo and Worst Case analyses can provide us with useful information concerning filter properties. Specifications such as standard and maximum deviation of a filter transfer function seem to be much more reliable quantities than standard (total) sensitivity measures (e.g. [19]) to say how deviations of filter element values influence filter properties. However, statistical analysis is a very time consuming task, especially for high-order filters. The aim of this work is to develop an efficient method of tolerance analysis of G_m-C filters. The novelty of the approach follows by utilising the matrix description of general structure of G_m-C filter described in recent papers (cf. [22], [23]). At the expense of limiting the deviations of filter element values, we get a very fast procedure which is characterised by low computational complexity and applicability to any structure of G_m-C filter of arbitrary order.

The paper is organised as follows. In Section 2, a general structure of G_m-C filter is presented. We discuss a matrix description of a general G_m-C filter based on a separate treatment of passive and active network of the circuit. In Section 3 we develop explicit formulas that allow us to calculate deviation of filter transfer function given deviations of its element values. At this stage the main equation describing the filter in Laplace transform domain is extended by adding auxiliary matrices containing deviations of filter element values. In the next step, linear approximation of extended equation is performed, which leads to the required formulas. A number of examples including comparison of the results provided by the approximate and exact method are presented in Section 4. Section 5 concludes the work.

2. GENERAL STRUCTURE OF G_m-C FILTER

Consider a general structure of a voltage-mode G_m-C filter shown in Fig.1. The current-mode counterpart can be obtained by inverting all transconductors and interchanging input and output of the filter [17],[18],[21]. The structure in Fig.1 contains n internal nodes denoted as x_i, $i = 1,...,n$, n input transconductors G_{mbi}, an output summer consisting of transconductors G_{mci} and $-G_{mo}$ as well as a feedforward transconductor G_{md}. All transconductors form *active network*, while input capacitors C_{bi}, $i = 1,...,n$ and capacitors C_{ij}, $1 \le i \le j \le n$ form *passive network*. It is easily seen that any G_m-C filter is a particular case of the general structure in Fig.1.

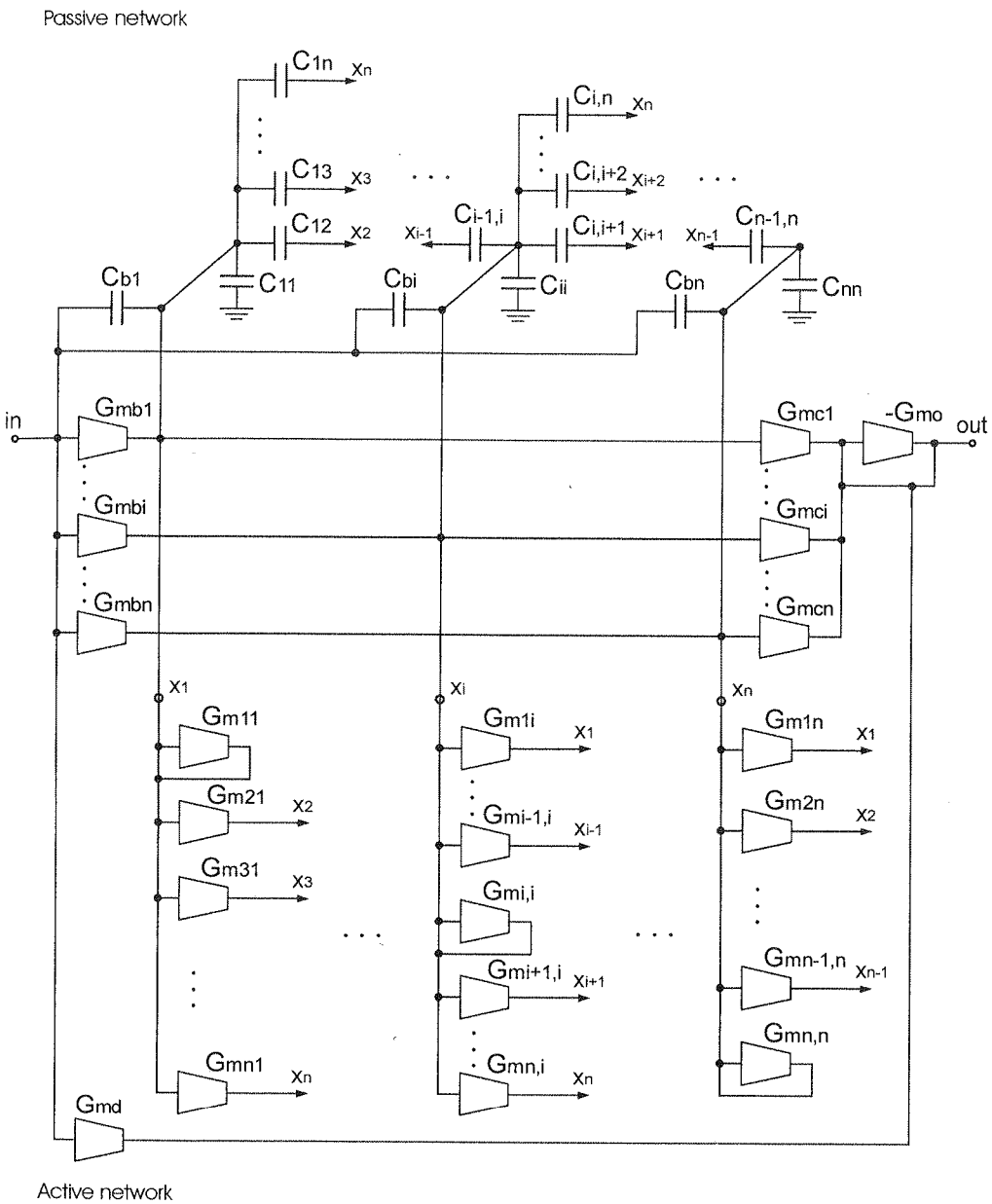

Fig. 1. General structure of voltage-mode G_m-C filter

Rys. 1. Ogólna struktura filtru G_m-C pracującego w trybie napięciowym

In the sequel we shall denote the voltage at the i-th node x_i also by x_i. A general structure of the voltage-mode G_m-C filter in Fig.1 can be described by the following matrix equations:

$$\begin{aligned} sT_C X &= GB + B^T u_i \\ u_o &= CX + Du_i \end{aligned} \tag{1}$$

where u_i, u_o are the input and output voltages, respectively, and

$$\mathbf{T}_C = \begin{bmatrix} C_{b1} + \sum_{j=1}^{n} C_{1j} & -C_{12} & \dots & -C_{1n} \\ -C_{12} & C_{b2} + \sum_{j=1}^{n} C_{2j} & \dots & -C_{2n} \\ \vdots & \vdots & \ddots & \vdots \\ -C_{1n} & -C_{2n} & \dots & C_{bn} + \sum_{j=1}^{n} C_{nj} \end{bmatrix},$$

$$\mathbf{G} = \begin{bmatrix} G_{m11} & G_{m12} & \dots & G_{m1n} \\ G_{m12} & G_{m22} & \dots & G_{m2n} \\ \vdots & \vdots & \ddots & \vdots \\ G_{mn1} & G_{mn2} & \dots & G_{mnm} \end{bmatrix}, \quad \mathbf{X} = \begin{bmatrix} x_1 \\ \vdots \\ x_n \end{bmatrix},$$

$$\begin{aligned} &\mathbf{B} = [G_{mb1} + sC_{b1} \quad \dots \quad G_{mbn} + sC_{bn}], \\ &\mathbf{C} = [c_1 \quad \dots \quad c_n], \quad c_i = G_{mci} / G_{mo}, \quad i = 1,2,\dots,n \\ &\mathbf{D} = d, \quad d = G_{md} / G_{mo} \end{aligned} \tag{2}$$

Note that T_C is a symmetrical matrix, i.e. $T_C^T = T_C$. On the basis of (1) we can calculate the filter transfer function:

$$H^{(0)}(s) = \frac{u_o(s)}{u_i(s)} = C(sT_C - \mathbf{G})^{-1} B^T + D \tag{3}$$

where index (0) refers to the fact that no filter element deviations have been taken into account. Now, let us denote adjoint matrix of $sT_C - G$ as $\tilde{A}$ where

$$\tilde{A}(s) = adj(sT_C - G) = [\tilde{A}_{ij}(s)]_{i,j=1}^{n} \tag{4}$$

This allows us to rewrite transfer function in the form:

$$\boldsymbol{H}^{(0)}(s) = \frac{1}{det(s\boldsymbol{T}_C - \boldsymbol{G})} \sum_{i,j=1}^{n} c_i (G_{mbj} + sC_{bj}) \tilde{A}_{ij}(s) + d \tag{5}$$

Note that many filter structures have only one input transconductor (i.e. no input signal distribution), a trivial output summer (i.e. one of the internal nodes is the output of the filter), and no input capacitors. This means that $\boldsymbol{B} = [0 \ \ldots \ 0 \ G_{mbk} \ 0 \ \ldots \ 0]$, $\boldsymbol{C} = [0 \ \ldots \ 0 \ 1 \ 0 \ \ldots \ 0]$ - 1 at l-th position and $C_{bi} = 0$ for $i = 0,1,\ldots n$. In such case, expression (5) reduces to the form:

$$\boldsymbol{H}^{(0)}(s) = \frac{G_{mbk} \tilde{A}_{lk}(s)}{det(s\boldsymbol{T}_C - \boldsymbol{G})} \tag{6}$$

Similar expression can be written for slightly more general case, with no input capacitors, input signal distribution (i.e. $\boldsymbol{B} = [G_{mb1} \ \ldots \ G_{mbn}]$), and a trivial output summer ($\boldsymbol{C} = [0 \ \ldots \ 0 \ 1 \ 0 \ \ldots \ 0]$ - 1 at l-th position). Then, we have

$$\boldsymbol{H}^{(0)}(s) = \frac{1}{det(s\boldsymbol{T}_C - \boldsymbol{G})} \sum_{i=1}^{n} G_{mbi} \tilde{A}_{li}(s) \tag{7}$$

On the basis of the above expressions one can easily calculate the transmittance of any particular structure of G_m-C filter. In a similar way one can treat current,,mode structures as well as state-space filters (see [22] for more details). It follows that the order n_H of transfer function of general filter structure in Fig.1 is not necessarily equal to the number of internal nodes. It can be shown that it essentially depends on the passive network. In particular, we have that n_H is not larger than the rank of the corresponding matrix $\boldsymbol{T}_C$.

3. TOLERANCE ANALYSIS OF G_m-C FILTERS

In this section we shall calculate the change of filter transfer function caused by the deviation of filter element values from their nominal values. We work within the setting of matrix description established in the previous section. Thus, we will consider the following deviation matrices:

$$\boldsymbol{T}_{\Delta C} = \begin{bmatrix} \Delta C_{b1} + \sum_{j=1}^{n} \Delta C_{1j} & -\Delta C_{12} & \ldots & -\Delta C_{1n} \\ -\Delta C_{12} & \Delta C_{b2} + \sum_{j=1}^{n} \Delta C_{2j} & \ldots & -\Delta C_{2n} \\ \vdots & \vdots & \ddots & \vdots \\ -\Delta C_{1n} & -\Delta C_{2n} & \ldots & \Delta C_{bn} + \sum_{j=1}^{n} \Delta C_{nj} \end{bmatrix},$$

$$G_\Delta = \begin{bmatrix} \Delta G_{m11} & \Delta G_{m12} & \dots & \Delta G_{m1n} \\ \Delta G_{m21} & \Delta G_{m22} & \dots & \Delta G_{m2n} \\ \vdots & \vdots & \ddots & \vdots \\ \Delta G_{mn1} & \Delta G_{mn2} & \dots & \Delta G_{mnn} \end{bmatrix}, \quad \begin{aligned} B_\Delta &= [\Delta G_{mb1} + s\Delta C_{b1} \dots \Delta G_{mbn} + s\Delta C_{bn}], \\ C_\Delta &= [\Delta c_1 \dots \Delta c_n], \\ D_\Delta &= \Delta d, \end{aligned} \quad (8)$$

where ΔG_{mij}, $i,j=1,\dots,n$, ΔG_{mbi}, $i=1,\dots,n$, ΔC_{ij}, $i,j=1,\dots,n$, $i\leq j$, ΔC_{bi}, $i=1,\dots,n$, Δc_i, $i=1,\dots,n$, Δd, denote deviation of transconductance values, capacitance values and summation coefficients, respectively. Obviously, we have $\Delta c_i = (G_{mo} \cdot \Delta G_{mci} - \Delta G_{mo} \cdot G_{mci})/G_{mo}^2$, $i=1,\dots,n$, and $\Delta d = (G_{mo} \cdot \Delta G_{md} - \Delta G_{mo} \cdot G_{md})/G_{mo}^2$. Taking into account (8), we modify the original equations (1) describing the filter so that they take the following form:

$$\begin{aligned} s(\boldsymbol{T}_C + \boldsymbol{T}_{\Delta C})\boldsymbol{X} &= (\boldsymbol{G} + \boldsymbol{G}_\Delta)\,\boldsymbol{X} + (\boldsymbol{B} + \boldsymbol{B}_\Delta)^T u_i \\ u_o &= (\boldsymbol{C} + \boldsymbol{C}_\Delta)\boldsymbol{X} + (\boldsymbol{D} + \boldsymbol{D}_\Delta)\,u_i \end{aligned}, \quad (9)$$

Using the first equation in (9) we can calculate the vector of node voltages $\boldsymbol{X}$ as:

$$\begin{aligned} \boldsymbol{X} &= [(s\boldsymbol{T}_C - \boldsymbol{G}) + (s\boldsymbol{T}_{\Delta C} - \boldsymbol{G}_\Delta)]^{-1}\,(\boldsymbol{B} + \boldsymbol{B}_\Delta)^T u_i \\ &= [(s\boldsymbol{T}_C - \boldsymbol{G})(\boldsymbol{I} + (s\boldsymbol{T}_C - \boldsymbol{G})^{-1}\,(s\boldsymbol{T}_{\Delta C} - \boldsymbol{G}_\Delta))]^{-1}\,(\boldsymbol{B} + \boldsymbol{B}_\Delta)^T u_i \\ &= [\boldsymbol{I} + (s\boldsymbol{T}_C - \boldsymbol{G})^{-1}\,(s\boldsymbol{T}_{\Delta C} - \boldsymbol{G}_\Delta)]^{-1}\,(s\boldsymbol{T}_C - \boldsymbol{G})^{-1}\,(\boldsymbol{B} + \boldsymbol{B}_\Delta)^T u_i \end{aligned} \quad (10)$$

Here, $\boldsymbol{I}$ stands for the identity matrix. For the rest of the paper we shall assume that element deviations are small. This means, in particular, that the norm of matrix $(s\boldsymbol{T}_C - \boldsymbol{G})^{-1}\,(s\boldsymbol{T}_{\Delta C} - \boldsymbol{G}_\Delta)$ is small, so we can use the following approximation

$$(\boldsymbol{I} + \boldsymbol{A})^{-1} \approx \boldsymbol{I} - \boldsymbol{A}, \quad (11)$$

which holds for any matrix $\boldsymbol{A}$ such that $\|\boldsymbol{A}\| \ll 1$. Using (11) we obtain

$$\boldsymbol{X} \cong [\boldsymbol{I} - (s\boldsymbol{T}_C - \boldsymbol{G})^{-1}\,(s\boldsymbol{T}_{\Delta C} - \boldsymbol{G}_\Delta)](s\boldsymbol{T}_C - \boldsymbol{G})^{-1}\,(\boldsymbol{B} + \boldsymbol{B}_\Delta)^T u_i \quad (12)$$

Hence, the filter transfer function at the presence of element deviations is given by the following formula

$$\boldsymbol{H}(s) = (\boldsymbol{C} + \boldsymbol{C}_\Delta)[\boldsymbol{I} - (s\boldsymbol{T}_C - \boldsymbol{G})^{-1}\,(s\boldsymbol{T}_{\Delta C} - \boldsymbol{G}_\Delta)](s\boldsymbol{T}_C - \boldsymbol{G})^{-1}\,(\boldsymbol{B} + \boldsymbol{B}_\Delta)^T + \boldsymbol{D} + \boldsymbol{D}_\Delta. \quad (13)$$

By neglecting all higher order terms with respect to deviation we get

$$\begin{aligned} \boldsymbol{H}(s) = {} & \boldsymbol{C}(s\boldsymbol{T}_C - \boldsymbol{G})^{-1}\,\boldsymbol{B}^T + \boldsymbol{C}(s\boldsymbol{T}_C - \boldsymbol{G})^{-1}\,\boldsymbol{B}_\Delta^T + \boldsymbol{C}_\Delta\,(s\boldsymbol{T}_C - \boldsymbol{G})^{-1}\boldsymbol{B}^T \\ & + \boldsymbol{D} + \boldsymbol{D}_\Delta - \boldsymbol{C}(s\boldsymbol{T}_C - \boldsymbol{G})^{-1}\,(s\boldsymbol{T}_{\Delta C} - \boldsymbol{G}_\Delta)(s\boldsymbol{T}_C - \boldsymbol{G})^{-1}\boldsymbol{B}^T \end{aligned} \quad (14)$$

Introducing matrices $\boldsymbol{C}_L$ and $\boldsymbol{C}_R$ defined as follows

$$\boldsymbol{C}_L = \boldsymbol{C}(s\boldsymbol{T}_C - \boldsymbol{G})^{-1}, \qquad \boldsymbol{C}_R = (s\boldsymbol{T}_C - \boldsymbol{G})^{-1}\boldsymbol{B}^T, \tag{15}$$

we can rewrite (14) as

$$\boldsymbol{H}(s) = \boldsymbol{C}_L\,(\boldsymbol{B}^T + \boldsymbol{B}_\Delta^T) + \boldsymbol{C}_\Delta\boldsymbol{C}_R + \boldsymbol{D} + \boldsymbol{D}_\Delta - \boldsymbol{C}_L\,(s\boldsymbol{T}_{\Delta C} - \boldsymbol{G}_\Delta)\boldsymbol{C}_R. \tag{16}$$

Now, using (3) and (16), we can calculate the transfer function deviation $\Delta\boldsymbol{H}(s) = \boldsymbol{H}(s) - \boldsymbol{H}^{(0)}(s)$:

$$\Delta\boldsymbol{H}(s) = \boldsymbol{C}_L\boldsymbol{B}_\Delta^T + \boldsymbol{C}_\Delta\boldsymbol{C}_R - \boldsymbol{C}_L\,(s\boldsymbol{T}_{\Delta C} - \boldsymbol{G}_\Delta)\,\boldsymbol{C}_R + \boldsymbol{D}_\Delta, \tag{17}$$

the amplitude deviation of the transfer function $\Delta\,|\,\boldsymbol{H}(s)\,| = |\,\boldsymbol{H}(s)\,| - |\,\boldsymbol{H}^{(0)}\,(s)$:

$$\Delta\,|\,\boldsymbol{H}(s)\,| = |\,\boldsymbol{C}_L\,(\boldsymbol{B}^T + \boldsymbol{B}_\Delta^T) + \boldsymbol{C}_\Delta\boldsymbol{C}_R - \boldsymbol{C}_L(s\boldsymbol{T}_{\Delta C} - \boldsymbol{G}_\Delta)\boldsymbol{C}_R + \boldsymbol{D} + \boldsymbol{D}_\Delta\,| - |\,\boldsymbol{C}_L\boldsymbol{B}_\Delta^T + \boldsymbol{D}\,|, \tag{18}$$

or phase deviation of the transfer function $\Delta(\arg\,\boldsymbol{H}(s)) = \arg\,\boldsymbol{H}(s) - \arg\,\boldsymbol{H}^{(0)}\,(s)$

$$\Delta(\arg\,\boldsymbol{H}(s)) = \arg(\boldsymbol{C}_L(\boldsymbol{B}^T + \boldsymbol{B}_\Delta^T) + \boldsymbol{C}_\Delta\boldsymbol{C}_R - \boldsymbol{C}_L\,(s\boldsymbol{T}_{\Delta C} - \boldsymbol{G}_\Delta)\boldsymbol{C}_R + \boldsymbol{D} + \boldsymbol{D}_\Delta) - \arg(\boldsymbol{C}_L\boldsymbol{B}_\Delta^T + \boldsymbol{D}). \tag{19}$$

Obviously, formula (17) is nothing else but the differential of $\boldsymbol{H}(s)$, i.e.

$$\Delta\boldsymbol{H}(s) = \sum_{i=1}^{N} \frac{\partial\boldsymbol{H}(s)}{\partial z_i}\,\Delta z_i \tag{20}$$

where z_i denote filter elements (i.e. capacitors and transconductors). Expression (17) is just a very convenient way to calculate it.

Note that if we assume trivial output summer ($\boldsymbol{C}$ = [0 ... 0 1 0 ...0]- 1 at l-th position), then we have $\boldsymbol{C}_\Delta = 0$ and $\boldsymbol{D}_\Delta = 0$ and (17), (18) and (19) simplify to

$$\Delta\boldsymbol{H}(s) = \boldsymbol{C}_L[\boldsymbol{B}_\Delta^T - (s\boldsymbol{T}_{\Delta C} - \boldsymbol{G}_\Delta)\boldsymbol{C}_R], \tag{21}$$

$$\Delta\,|\,\boldsymbol{H}(s)\,| = |\,\boldsymbol{C}_L\,(\boldsymbol{B} + \boldsymbol{B}_\Delta^T) - \boldsymbol{C}_L\,(s\boldsymbol{T}_{\Delta C} - \boldsymbol{G}_\Delta)\boldsymbol{C}_R + \boldsymbol{D}\,| - |\,\boldsymbol{C}_L\boldsymbol{B}_\Delta^T + \boldsymbol{D}\,|, \tag{22}$$

$$\Delta(\arg\,\boldsymbol{H}(s)) = \arg(\boldsymbol{C}_L(\boldsymbol{B}^T + \boldsymbol{B}_\Delta^T) - \boldsymbol{C}_L(s\boldsymbol{T}_{\Delta C} - \boldsymbol{G}_\Delta)\boldsymbol{C}_R + \boldsymbol{D}) - \arg(\boldsymbol{C}_L\boldsymbol{B}_\Delta^T + \boldsymbol{D}). \tag{23}$$

It is seen that the above formulas are very simple and general, since they allow us to analyse an arbitrary G_m-C filter structure. Due to the fact that they use a matrix formulation, it is easy to implement computer software to evaluate these formulas in a very efficient way. In particular, one can perform a very fast Monte Carlo and/or Worst Case analysis. Note that matrices $\boldsymbol{C}_L$ and $\boldsymbol{C}_R$ have to be calculated only once for a given filter structure. Then, the evaluation of formulas (17)-(19) (or (21)-(23)) is nothing else but a simple matrix (or vector) multiplication, no matter how we change the deviation of the filter element values.

There is no need to invert the matrix $s(\boldsymbol{T}_C+\boldsymbol{T}_{\Delta C})-(\boldsymbol{G}+\boldsymbol{G}_\Delta)$ while changing these deviations. Due to this fact a computational cost of determining transfer function deviation using approximate formulas is only $O(n^2)$. For example, an analysis of 8th order filter is about five times faster than the same analysis being done using the exact method.

In the case of low order filters it is possible to perform hand tolerance analysis. For illustration purposes consider a second-order G_m-C filter shown in Fig.2. We shall assume for simplicity that nominal values of all filter transconductors are the same (up to the sign), i.e. $G_{b1}=G_{21}=-G_{12}=-G_{22}=g$, while element deviations will be denoted as ΔC_1, ΔC_2, ΔG_{b1}, ΔG_{21}, ΔG_{12}, ΔG_{22}. The matrices describing this filter are

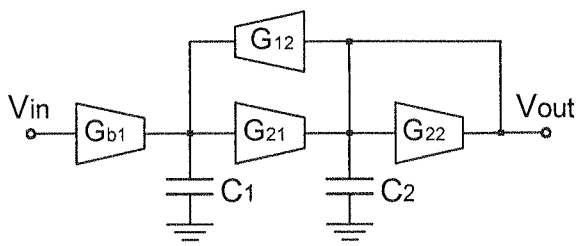

Fig.2. Diagram of the second,,order low,,pass Gm,,C filter

Rys.2. Schemat dolnoprzepustowego filtru Gm,,C drugiego rzędu

$$\boldsymbol{T}_C=\begin{bmatrix} C_1 & 0 \\ 0 & C_2 \end{bmatrix},\ \boldsymbol{G}=\begin{bmatrix} 0 & -g \\ g & -g \end{bmatrix},\ \boldsymbol{B}=[g \quad 0],\ \boldsymbol{C}=[0 \quad 1],\ \boldsymbol{D}=0. \tag{24}$$

Using (24) one can easily calculate matrices $\boldsymbol{C}_L$ and $\boldsymbol{C}_R$ that are

$$\boldsymbol{C}_L=\frac{1}{D(s)}[g \quad sC_1],\qquad \boldsymbol{C}_R=\frac{1}{D(s)}\begin{bmatrix} sC_2g+g^2 \\ g^2 \end{bmatrix}, \tag{25}$$

with

$$\boldsymbol{D}(s)=C_1C_2s^2+C_1gs+g^2. \tag{26}$$

Moreover, it follows from (3) that

$$\boldsymbol{H}^{(0)}(s)=\frac{g^2}{C_1C_2s^2+C_1gs+g^2}. \tag{27}$$

Now, using (21) we can calculate $\Delta\boldsymbol{H}(s)=\boldsymbol{H}(s)-\boldsymbol{H}^{(0)}(s)$, which is

$$\Delta\boldsymbol{H}(s)=\frac{1}{D(s)}[g \quad sC_1]\left(\begin{bmatrix} \Delta G_{b1} \\ 0 \end{bmatrix}-\frac{1}{D(s)}\begin{bmatrix} s\Delta C_1 & -\Delta G_{12} \\ \Delta G_{21} & s\Delta C_2-\Delta G_{22} \end{bmatrix}\begin{bmatrix} sC_2g+g^2 \\ g^2 \end{bmatrix}\right) \tag{28}$$

Hence, we get

$$\Delta \boldsymbol{H}(s) = \frac{g}{D^2(s)}[-s(sC_2 + g)\Delta C_1 + s^2 C_1 g \Delta C_2 + g^2 \Delta G_{12} - sC_1(sC_2 + g)\Delta G_{21} + sC_1 g \Delta G_{22} + D(s)\Delta G_{b1}]. \tag{29}$$

In a similar way one can calculate explicit formulas for $\Delta|\boldsymbol{H}(s)|$ and $\Delta(\arg \boldsymbol{H}(s))$.

4. APPLICATION EXAMPLES

In this section we consider several application examples of a tolerance analysis method introduced in the previous section. Throughout this section we shall use normalised element values and normalised frequency. All the results of Monte Carlo simulations have been obtained on the basis of 5000 random samples. The standard deviation of amplitude and phase, used in the sequel, are defined as

$$S_{|H(j\omega)|} = \sqrt{\frac{1}{n-1}\sum_{i=1}^{n}(|H_i(j\omega)| - |H^{(0)}(j\omega)|)^2} \tag{30}$$

$$S_{\arg H(j\omega)} = \sqrt{\frac{1}{n-1}\sum_{i=1}^{n}(\arg H_i(j\omega) - H^{(0)}(j\omega))^2} \tag{31}$$

where $|H^{(0)}(j\omega)|$ ($\arg H^{(0)}(j\omega)$) is the nominal amplitude (phase) and $|H_i(j\omega)|$ ($\arg H_i(j\omega)$) is the actual amplitude (phase) for i-th random sample. We have assumed a gaussian distribution of the deviations of filter element values while calculating standard deviations (30), (31) and a flat distribution while calculating maximum deviations of amplitude and phase. In figures containing the results of the statistical simulations solid lines show the results achieved according to approximate formulas (22) and (23); points indicate the results obtained according to the exact formulas based on equation (9). Deviations of amplitude and phase are calculated in dB and degrees, respectively.

As the first example, consider again a second-order filter in Fig.2. We assume that this filter implements Butterworth transfer function. Then, the normalised element values are: C_1=1.4142, C_2=0.7071, G_{b1}=G_{21}=1.0, G_{12}=G_{22}=-1.0. Figs.3 and 4 show the modulus and phase of the nominal transfer function of the filter, respectively. Figs.5,6 (Figs.7,8) show the results of Monte Carlo simulation (Worst Case analysis) of amplitude and phase of the transfer function. We have assumed 1%, 2%, 5% and 10% deviations for all filter elements. Figs.5 and 6 show standard deviation of amplitude and phase, respectively. Figs.7 and 8 show maximum deviation of amplitude and phase, respectively. One can infer from the data in Figs.5–8 that formulas (22), (23) provide us with a very good approximation. Standard deviation calculated by means of both methods is almost identical even for the deviations in filter element values equal to 10%. The results are slightly worse for

maximum deviations, however, the error is negligible for deviations of element values smaller or equal to 5%.

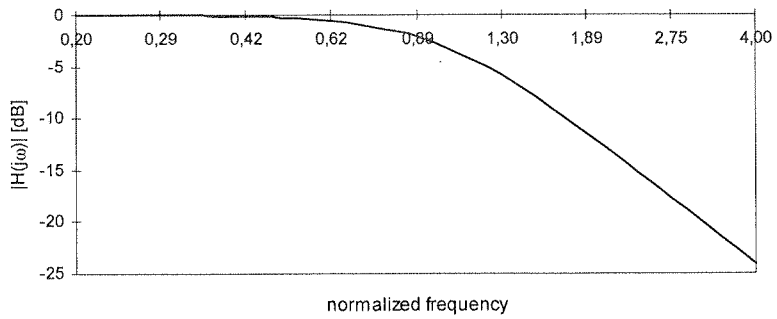

Fig. 3. Nominal amplitude characteristic |H(jω)| of 2nd order Butterworth filter in Fig. 2

Rys. 3. Nominalna charakterystyka amplitudowa |H(jω)| filtru Butterwortha 2-go rzędu z Rys. 2

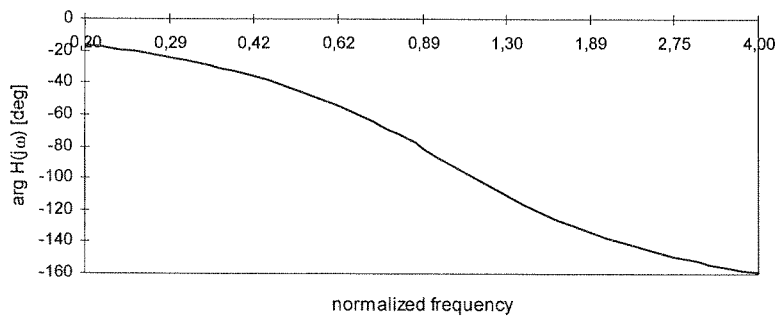

Fig. 4. Nominal phase charasteristic arg[H(jω)] of 2nd ordr Buttrworth filtr in Fig. 2

Rys. 4. Nominalna charakterystyka fazowa arg[H(jω)] filtru Butterwortha 2-go rzędu z Rys. 2

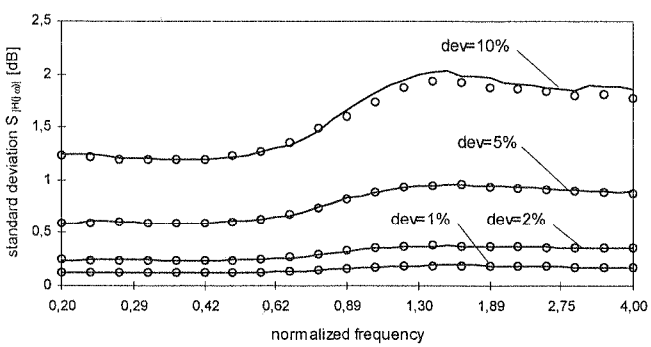

Fig. 5. Standard deviation of amplitude $S_{|H(j\omega)|}$ versus normalised frequency for 2nd order Butterworth filter in Fig. 2 with a deviation in filter element values as a parameter; approximate values denoted as solid line and exact values as circles; gaussian distribution in element values was assumed

Rys. 5. Odchylenie standardowe amplitudy $S_{|H(j\omega)|}$ w funkcji znormalizowanej częstotliwości dla filtru Butterwortha 2-go rzędu z Rys. 2 z odchyłką wartości elementów jako parametrem; wartości przybliżone oznaczono linią ciągłą, wartości dokładne oznaczono punktami; przyjęto gaussowski rozkład odchyłek wartości elementów

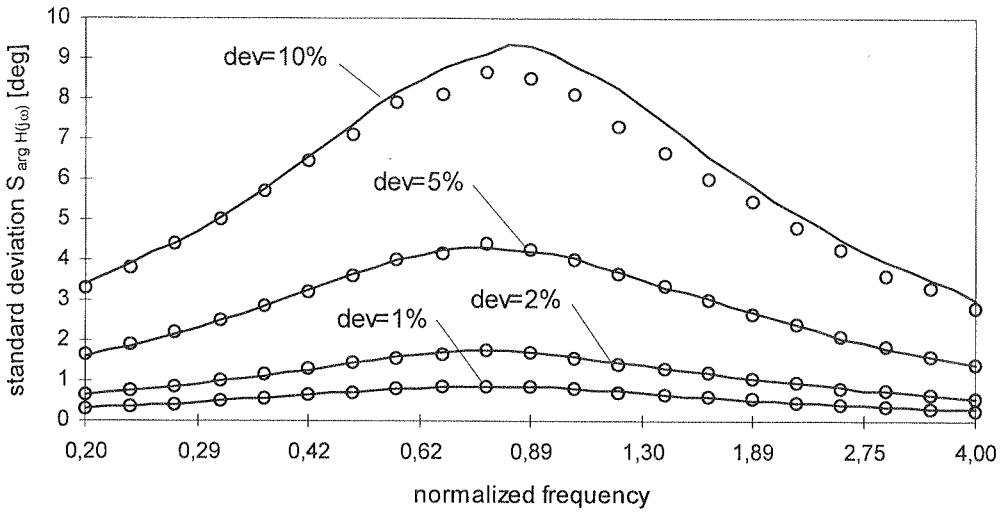

Fig. 6. Standard deviation of phase $S_{\arg H(j\omega)}$ versus normalised frequency for 2nd order Butterworth filter in Fig. 2 with a deviation in filter element values as a parameter; approximate values denoted as solid line and exact values as circles; gaussian distribution in element values was assumeed

Rys. 6. Odchylenie standardowe fazy $S_{\arg H(j\omega)}$ w funkcji znormalizowanej częstotliwości dla filtru Butterwortha 2-go rzędu z Rys. 2 z odchyłką wartości elementów jako parametrem; wartości przybliżone oznaczono linią ciągłą, wartości dokładne oznaczono punktami; przyjęto gaussowski rozkład odchyłek wartości elementów

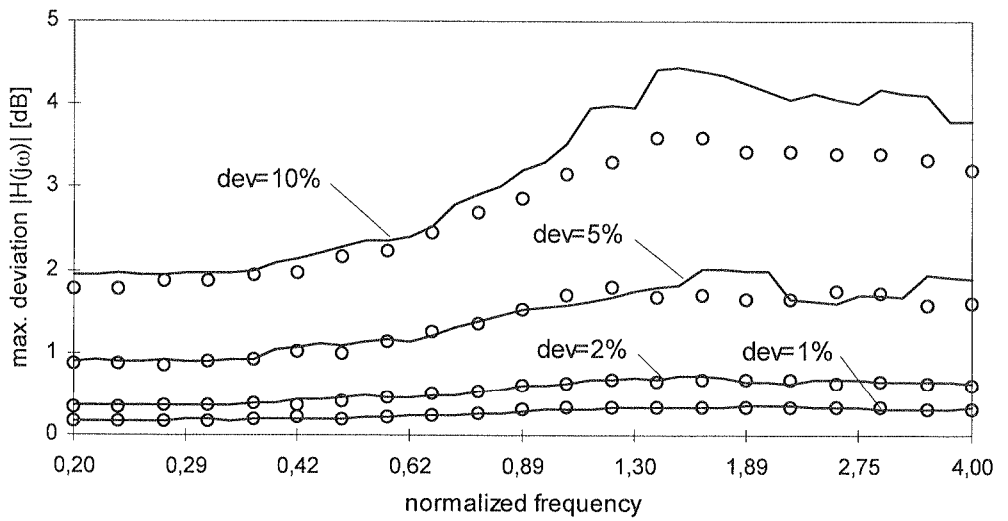

Fig. 7. Maximum deviation of amplitude versus normalised frequency for 2nd order Butterworth filter in Fig. 2 with a deviation in filter element values as a parameter; approximate values denoted as solid line and exact values as circles; flat distribution in element values was assumed

Rys. 7. Odchylenie maksymalne amplitudy w funkcji znormalizowanej częstotliwości dla filtru Butterwortha 2-go rzędu z Rys. 2 z odchyłką wartości elementów jako parametrem; wartości przybliżone oznaczono linią ciągłą, wartości dokładne oznaczono punktami; przyjęto jednostajny rozkład odchyłek wartości elementów

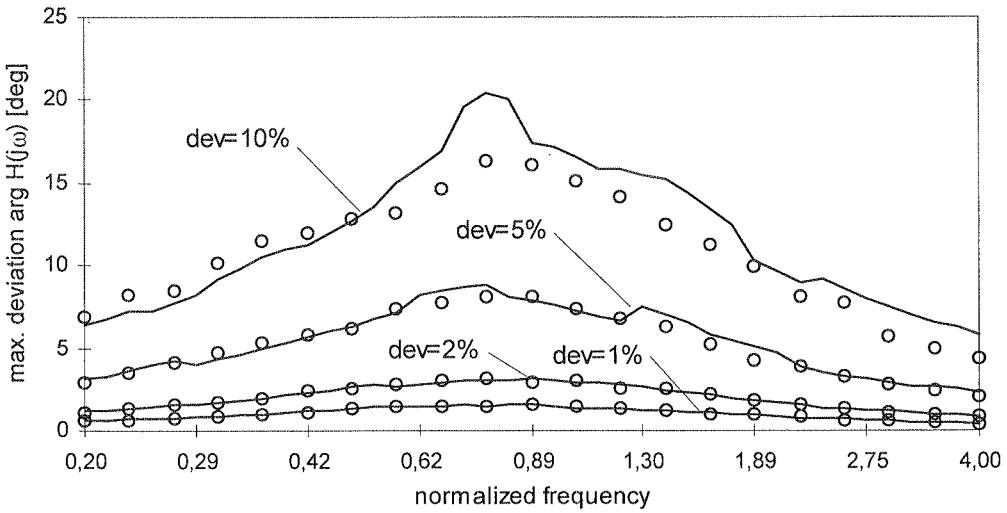

Fig. 8. Maximum deviation of phase versus normalised frequency for 2nd order Butterworth filter in Fig. 2 with a deviation in filter element values as a parameter; approximate values denoted as solid line and exact values as circles; flat distribution in element values was assumed

Rys. 8. Odchylenie maksymalne amplitudy w funkcji znormalizowanej częstotliwości dla filtru Butterwortha 2-go rzędu z Rys. 2 z odchyłką wartości elementów jako parametrem; wartości przybliżone oznaczono linią ciągłą, wartości dokładne oznaczono punktami; przyjęto jednostajny rozkład odchyłek wartości elementów

Another example is a 3rd order elliptic low-pass filter in leap-frog (LF) structure with a floating capacitor [24] shown in Fig.9. We assume that the filter implements transfer function with minimum pass,,band attenuation A_1=0.9, maximum stop-band attenuation A_2=0.16 and selectivity ω_s/ω_p=1.2 [24]. The normalised filter element values in this case are: C_1=1.1653, C_2=0.6241, C_3=0.4710, C_4=0.9428, $G_{b1}=G_{21}=G_{32}$=1.0, $G_{12}=G_{23}=G_{33}$=-1.0.

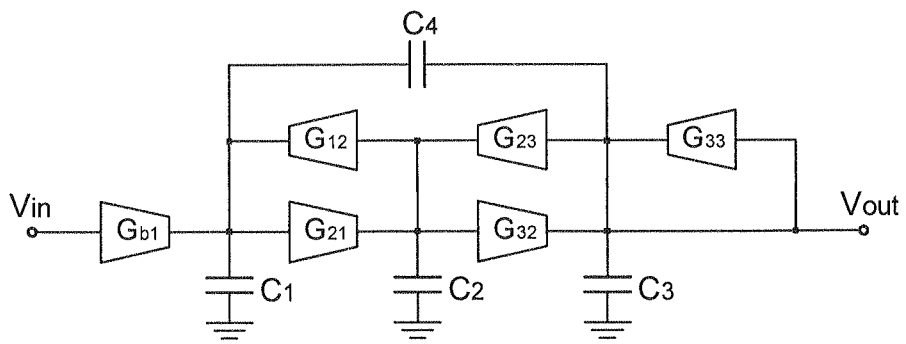

Fig. 9. A third order low-pass eliptic filter in LF structure with a floating capacitor

Rys. 9. Dolnoprzepustowy filtr eliptyczny trzeciego rzędu w strukturze LF z kondensatorem nieuziemionym

Figs.10 and 11 show the modulus and phase of the nominal transfer function of the filter, respectively. Figs.12,13 (Figs.14,15) show the results of Monte Carlo simulation (Worst Case analysis) of amplitude and phase of the transfer function. We have assumed 1%, 2%, 5% and 10% deviations for all filter elements. Figs.12 and 13 show standard deviation of amplitude and phase, respectively. Figs.14 and 15 show maximum deviation of amplitude and phase, respectively. It follows from the data in Figs.12–15 that formulas (22), (23) give a very good approximation for frequencies which are not too close to the frequency of the transmission zero of the filter. Standard deviation calculated by means of both methods is almost the same even for the deviation in filter element values equal to 10%. The results for maximum deviation are slightly worse. However, for frequencies close to the frequency of the transmission zero, approximation is not that good, especially for deviations of element values equal to or higher than 5%. We can account for this fact by recalling that $|H(j\omega)|$ decreases to minus infinity (in dB scale) as the frequency approaches zero of the transfer function. Thus, even very small error produced by the approximate formula (22) in a linear scale, gives considerable error in a logarithmic scale. Similarly, the transfer function has a considerable phase jump at its zero, which means that the results of maximum phase deviation are not reliable for frequencies close to this frequency point and for large deviation of filter element values.

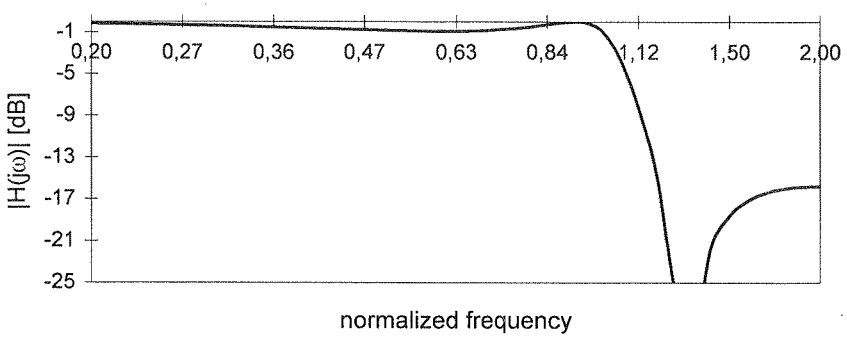

Fig. 10. Nominal amplitude characteristic |H(jω)| of 3rd order eliptic filter in Fig. 9

Rys. 10. Nominalna charakterystyka amplitudowa |H(jω)| filtru eliptycznego 3-go rzędu z Rys. 9

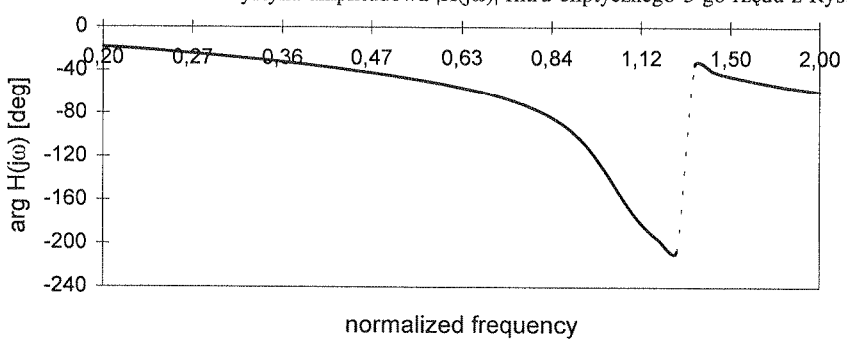

Fig. 11. Nominal phase characteristic arg[H(jω)] of 3rd order eliptic filter in Fig. 9

Rys. 11. Nominalna charakterystyka fazowa arg[H(jω)] filtru eliptycznego 3-go rzędu z Rys. 9

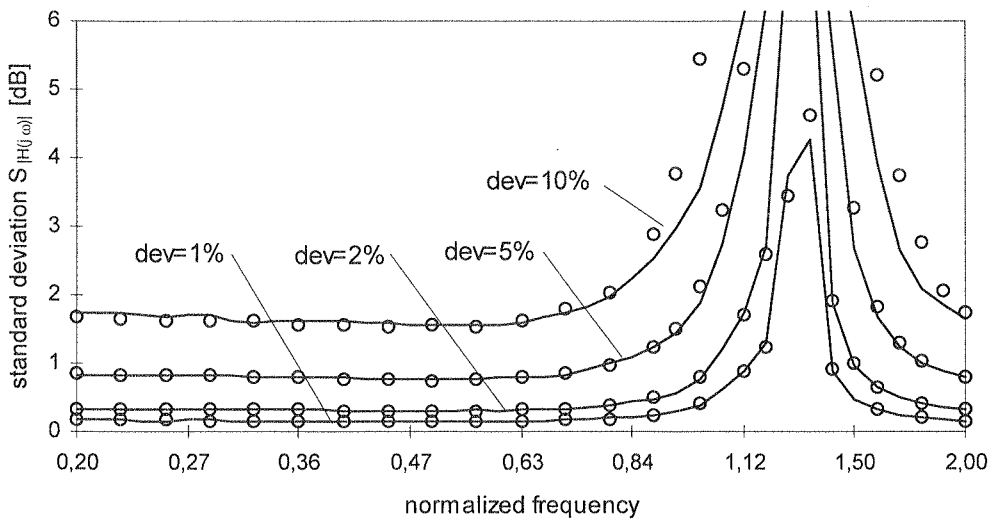

Fig. 12. Standard deviation of amplitude $S_{|H(j\omega)|}$ versus normalised frequncy for 3rd order eliptic filter in Fig. 9 with a deviation in filtr element valus as a parameter; approximate values denoted as solid line and exact values as circles; gaussian distribution in element values was assumed

Rys. 12. Odchylenie standardowe amplitudy $S_{|H(j\omega)|}$ w funkcji znormalizowanj częstotliwości dla filtru eliptycznego 3-go rzędu z Rys. 9 z odchyłką wartości elementów jako parametrem; wartości przybliżone oznaczono linią ciągłą, wartości dokładne oznaczono punktami; przyjęto gaussowski rozkład odchyłek wartości elementów

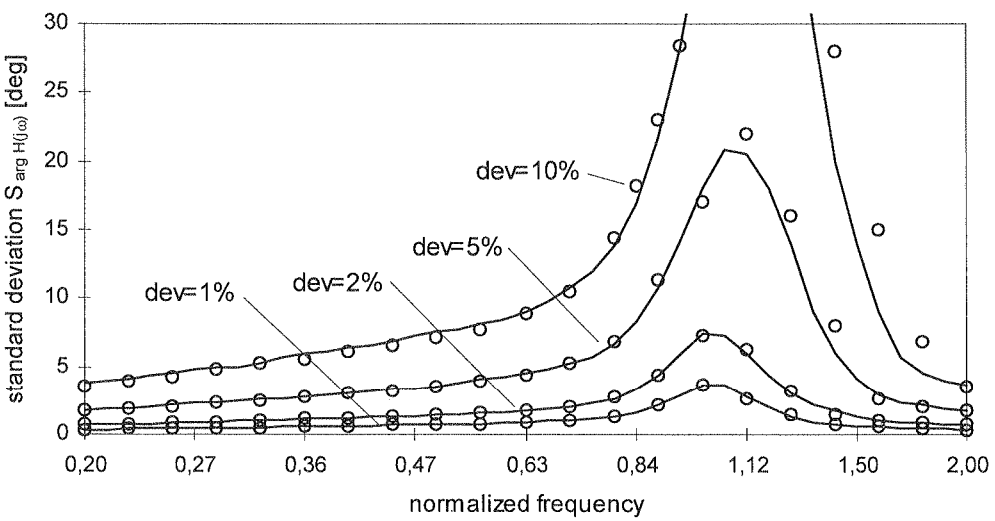

Fig. 13. Standard deviation of phase $S_{arg H(j\omega)}$ versus normalised frequncy for 3rd order eliptic filter in Fig. 9 with a deviation in filtr element values as a parameter; approximate values denoted as solid line and exact values as circles; gaussian distribution in element values was assumed

Rys. 13. Odchylenie standardowe fazy $S_{arg H(j\omega)}$ w funkcji znormalizowanj częstotliwości dla filtru eliptycznego 3-go rzędu z Rys. 9 z odchyłką wartości elementów jako parametrem; wartości przybliżone oznaczono linią ciągłą, wartości dokładne oznaczono punktami; przyjęto gaussowski rozkład odchyłek wartości elementów

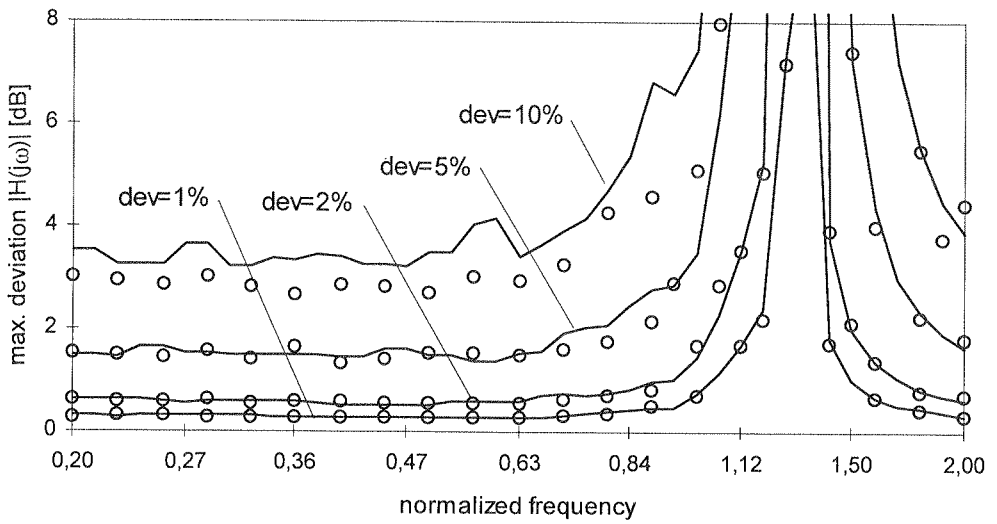

Fig. 14. Maximum deviation of amplitude versus normalised frequncy for 3rd order eliptic filter in Fig. 9 with a deviation in filtr element values as a parameter; approximate values denoted as solid line and exact values as circles; flat distribution in element values was assumed

Rys. 14. Odchylenie maksymalne amplitudy w funkcji znormalizowanj częstotliwości dla filtru eliptyczngo 3-go rzędu z Rys. 9 z odchyłką wartości elementów jako parametrem; wartości przybliżone oznaczono linią ciągłą, wartości dokładne oznaczono punktami; przyjęto jednostajny rozkład odchyłek wartości elementów

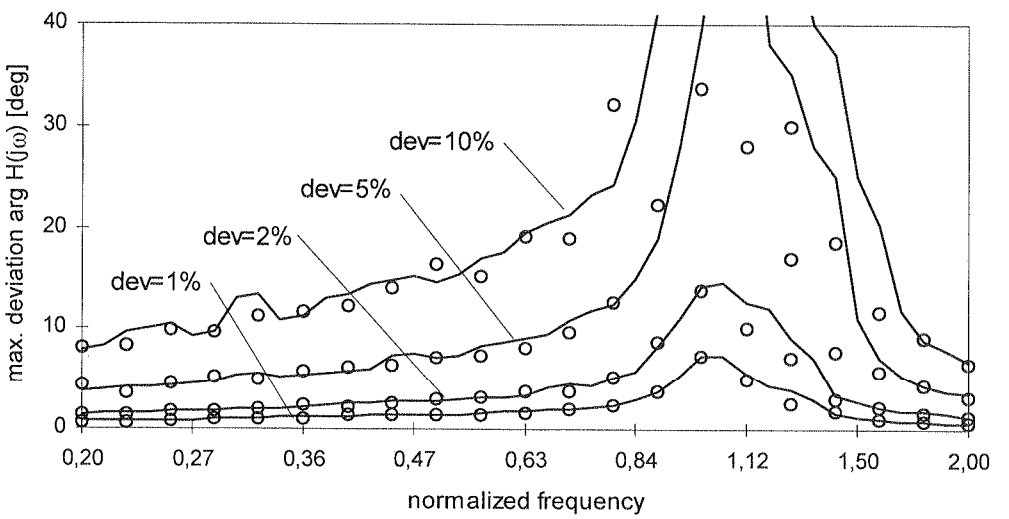

Fig. 15. Maximum deviation of phase versus normalised frequncy for 3rd order eliptic filter in Fig. 9 with a deviation in filter element values as a parameter; approximate values denoted as solid line and exact values as circles; flat distribution in element values was assumed

Rys. 15. Odchylenie maksymalne fazy w funkcji znormalizowanj częstotliwości dla filtru eliptyczngo 3-go rzędu z Rys. 9 z odchyłką wartości elementów jako parametrem; wartości przybliżone oznaczono linią ciągłą, wartości dokładne oznaczono punktami; przyjęto jednostajny rozkład odchyłek wartości elementów

Now, consider the all-pole low-pass LF filter that realizes 8th order Butterworth transfer function. A diagram of a general structure of all-pole low-pass IFLF filter is shown in Fig.16. Here, we have n=8. As before, we use normalised values of elements and normalised frequency. We assume that $G_{b1} = G_{i,i-1} = -G_{j8} = 1$, i=2,...,n, j=1,...,n, i.e. all transconductors are the same (up to the sign). Normalised values of capacitances are: C_1=1.560, C_2=1.827, C_3=1.729, C_4=1.526, C_5=1.259, C_6=0.937, C_7=0.578, C_8=0.195. Normalised value of corner frequency equals 1.

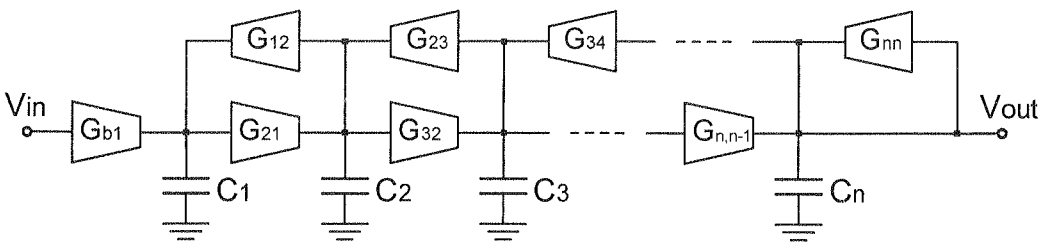

Fig. 16. Diagram of a n-th ordr all-pole low-pass LF filter structure

Rys. 16. Schemat filtru dolnoprzepustowego rzędu n w strukturze LF bez zer transmisyjnych

Figs.17 and 18 show the modulus and phase of the nominal transfer function of the filter, respectively. Figs.19,20 (Figs.21,22) show the results of Monte Carlo simulation (Worst Case analysis) of amplitude and phase of the transfer function. We have assumed 1%, 2%, 3% and 5% deviations for all filter elements. Figs.19 and 20 show standard deviation of amplitude and phase, respectively. Figs.21 and 22 show maximum deviation of amplitude and phase, respectively. Also in this case we can observe a very good agreement between the results obtained by means of the approximate and exact formulas.

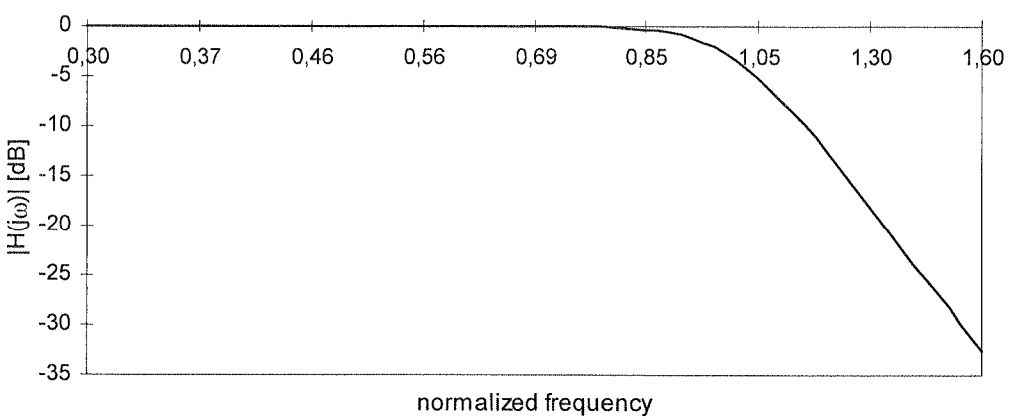

Fig. 17. Nominal amplitude characteristic |H(jω)| of 8th order Butterworth LF filtr in Fig. 16

Rys. 17. Nominalna charakterystyka amplitudowa |H(jω)| filtru Butterwortha 8-go rzędu z Rys. 16

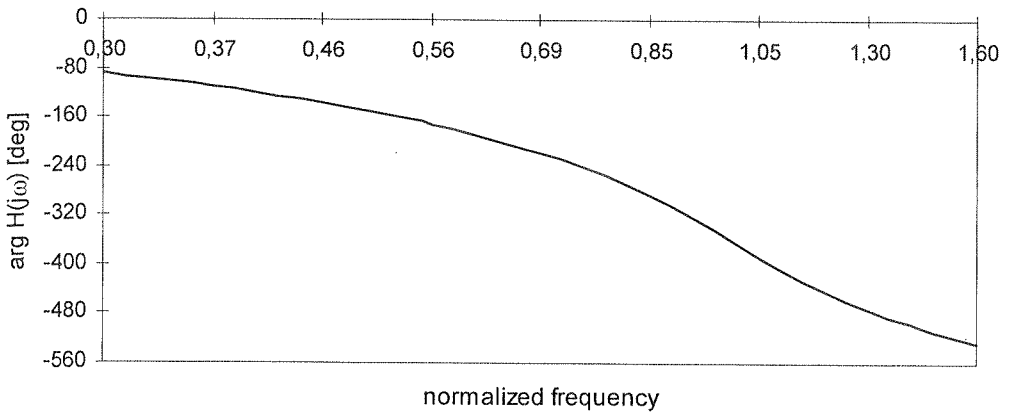

Fig. 18. Nominal phase characteristic arg[H(jω)] of 8th order Butterworth LF filter in Fig. 16

Rys. 18. Nominalna charakterystyka fazowa arg[H(jω)] filtru Butterwortha 8-go rzędu z Rys. 16

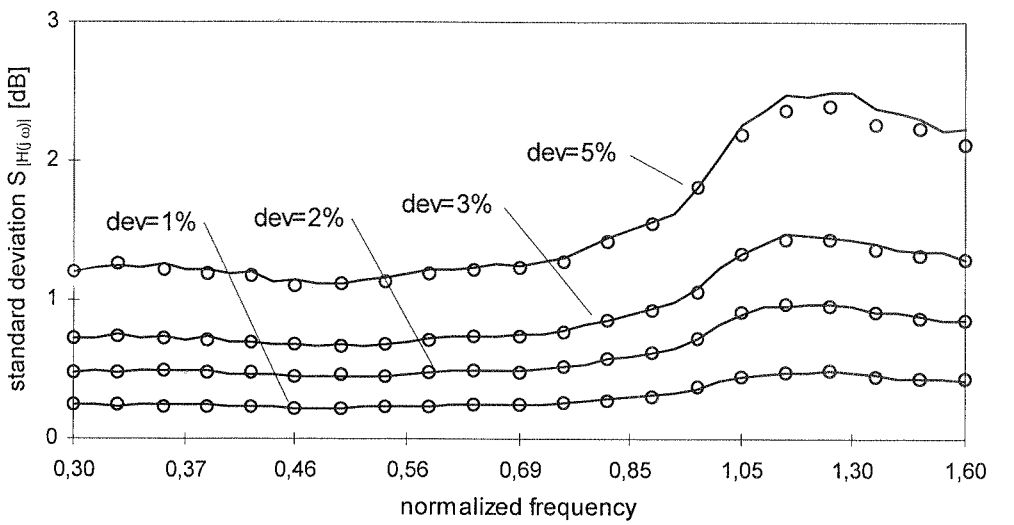

Fig. 19. Standard deviation of amplitude $S_{|H(j\omega)|}$ versus normalised frequency for 8th order Butterworth LF filter in Fig. 16 with a deviation in filter element values as a parameter; approximate values denoted as solid line and exact values as circles; gaussian distribution in element values was assumed

Rys. 19. Odchylenie standardowe amplitudy $S_{|H(j\omega)|}$ w funkcji znormalizowanej częstotliwości dla filtru Butterwortha 8-go rzędu z Rys. 16 z odchyłką wartości elementów jako parametrem; wartości przybliżone oznaczono linią ciągłą, wartości dokładne oznaczono punktami; przyjęto gaussowski rozkład odchyłek wartości elementów

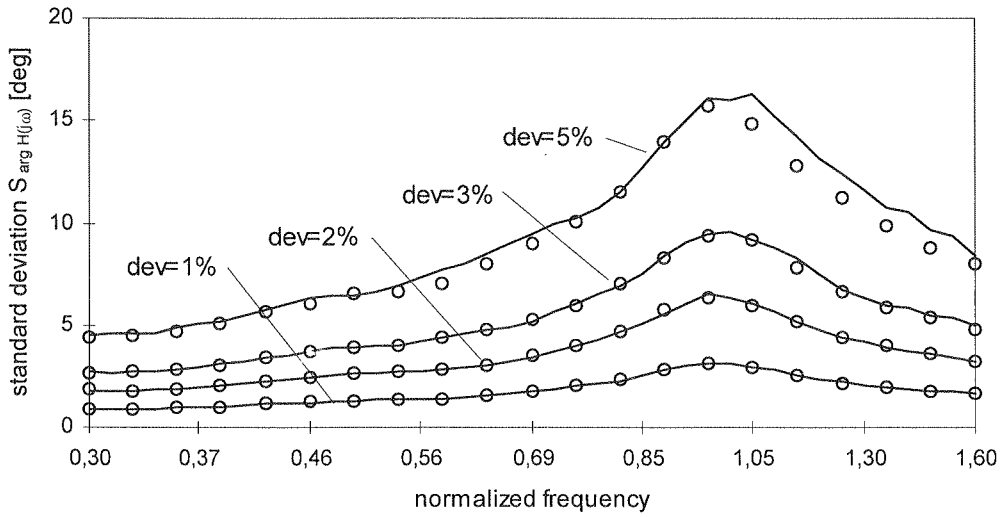

Fig. 20. Standard deviation of phase $S_{\arg H(j\omega)}$ versus normalised frequency for 8th order Butterworth LF filter in Fig. 16 with a deviation in filter element values as a parameter; approximate values denoted as solid line and exact values as circles; gaussian distribution in element values was assumed

Rys. 20. Odchylenie standardowe fazy $S_{\arg H(j\omega)}$ w funkcji znormalizowanej częstotliwości dla filtru Butterwortha 8-go rzędu z Rys. 16 z odchyłką wartości elementów jako parametrem; wartości przybliżone oznaczono linią ciągłą, wartości dokładne oznaczono punktami; przyjęto gaussowski rozkład odchyłek wartości elementów

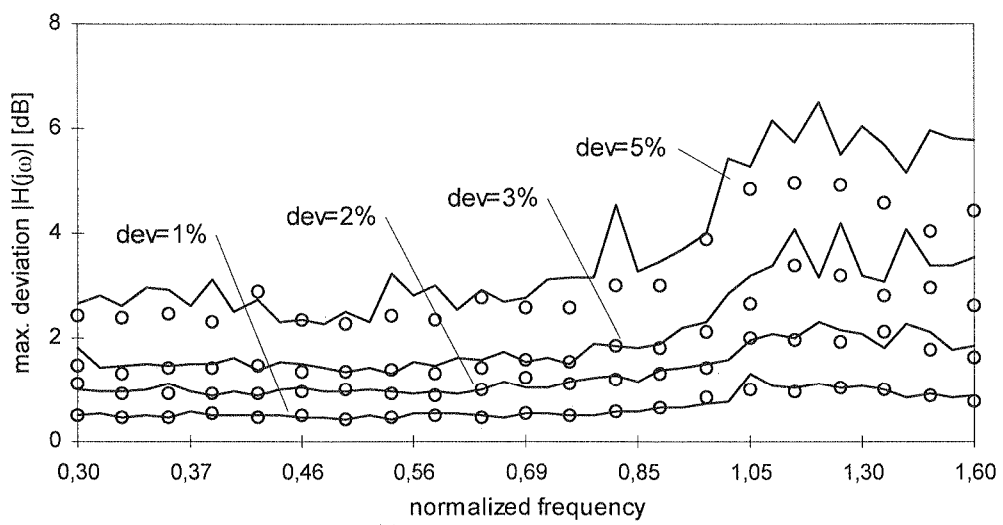

Fig. 21. Maximum deviation of amplitude versus normalised frequency for 8th order Butterworth LF filter in Fig. 16 with a deviation in filter element values as a parameter; approximate values denoted as solid line and exact values as circles; flat distribution in element values was assumed

Rys. 21. Odchylenie maksymalne amplitudy w funkcji znormalizowanej częstotliwości dla filtru Butterwortha 8-go rzędu z Rys. 16 z odchyłką wartości elementów jako parametrem; wartości przybliżone oznaczono linią ciągłą, wartości dokładne oznaczono punktami; przyjęto jednostajny rozkład odchyłek wartości elementów

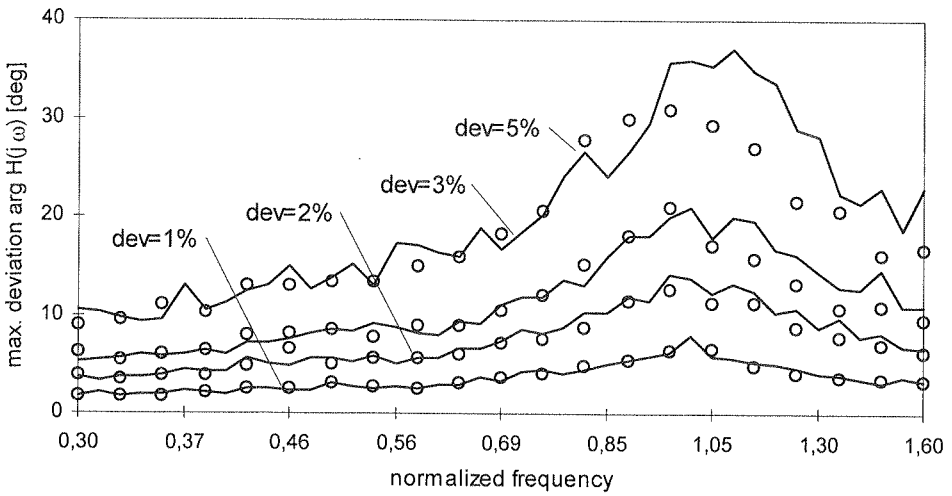

Fig. 22. Maximum deviation of phase versus normalised frequency for 8th order Butterworth LF filter in Fig. 16 with a deviation in filter element values as a parameter; approximate values denoted as solid line and exact values as circles; flat distribution in element values was assumed

Rys. 22. Odchylenie maksymalne fazy w funkcji znormalizowanej częstotliwości dla filtru Butterwortha 8-go rzędu z Rys. 16 z odchyłką wartości elementów jako parametrem; wartości przybliżone oznaczono linią ciągłą, wartości dokładne oznaczono punktami; przyjęto jednostajny rozkład odchyłek wartości elementów

Since the proposed method is very fast, it can be used to make a comparison of different filter structures. As an example we shall compare different structures of all-pole canonical low-pass G_m-C filters that realize the same transfer function. Fig.23 shows a general structure of n-th order all-pole canonical low-pass G_m-C filter.

If the feedback signal at intrinsic node x_i in Fig.23 is taken from the node x_{i+1} for i=1,2,...,n−1 and the node x_n has the inner feedback loop the we obtain so,,called leap-frog (LF) structure. If all feedback signals at nodes x_i, i=1,2,...,n are taken from the node x_n then we get so-called inverse follow-the-leader (IFLF) structure. It is well known that IFLF and LF filters can be considered as two 'extreme' canonical structures of all-pole filters [23]. In general, the feedback signal emerging at node x_i can be taken from node x_j with j=i+1,...,n. This yields the total number (n-1)! of different canonical multiple-loop integrator structures of order n.

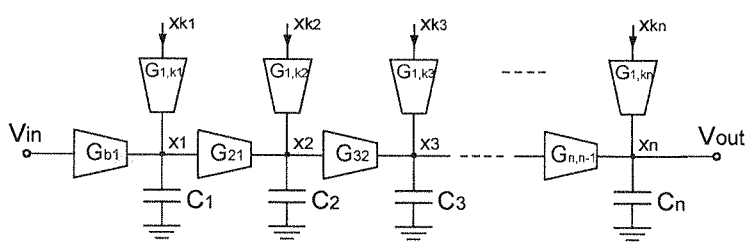

Fig. 23. A general structure of n-th order all-pole canonical low-pass G_m-C filter

Rys. 23. Ogólna struktura kanonicznego filtru dolnoprzepustowego G_m-C rzędu n bez zer transmisyjnych

Table 1

Standard deviation of amplitude for 5-th order all-pole low-pass Butterworth filters *

Odchylenie standardowe amplitudy dla dolnoprzepustowych filtrów Butterwortha 5-go rzędu

Filter structure	ω=0.5			ω=1.0			ω=2.0		
	G+C dev.	C dev.	G dev.	G+C dev.	C dev.	G dev.	G+C dev.	C dev.	G dev.
2 3 4 5 5	0.19	0.05	0.18	0.29	0.19	0.22	0.32	0.22	0.23
2 3 5 5 5	0.19	0.06	0.18	0.30	0.20	0.22	0.34	0.22	0.26
2 4 4 5 5	0.19	0.06	0.18	0.42	0.28	0.32	0.33	0.22	0.24
2 4 5 5 5	0.19	0.06	0.18	0.49	0.28	0.40	0.36	0.23	0.27
2 5 4 5 5	0.16	0.07	0.14	0.48	0.30	0.36	0.33	0.23	0.24
2 5 5 5 5	0.16	0.07	0.14	0.51	0.31	0.40	0.36	0.23	0.28
3 3 4 5 5	0.22	0.09	0.19	0.40	0.23	0.31	0.32	0.22	0.23
3 3 5 5 5	0.21	0.10	0.19	0.40	0.25	0.33	0.34	0.22	0.26
3 4 4 5 5	0.28	0.09	0.26	0.55	0.35	0.43	0.34	0.23	0.24
3 4 5 5 5	0.30	0.10	0.27	0.66	0.34	0.56	0.36	0.23	0.28
3 5 4 5 5	0.19	0.09	0.17	0.60	0.37	0.47	0.33	0.22	0.24
3 5 5 5 5	0.21	0.10	0.19	0.62	0.37	0.52	0.36	0.23	0.29
4 3 4 5 5	0.23	0.10	0.21	0.34	0.19	0.27	0.32	0.22	0.24
4 3 5 5 5	0.23	0.11	0.21	0.39	0.22	0.32	0.34	0.22	0.26
4 4 4 5 5	0.28	0.10	0.26	0.57	0.33	0.46	0.33	0.23	0.25
4 4 5 5 5	0.29	0.11	0.27	0.71	0.34	0.62	0.36	0.23	0.28
4 5 4 5 5	0.21	0.10	0.19	0.60	0.36	0.49	0.33	0.23	0.24
4 5 5 5 5	0.22	0.11	0.20	0.67	0.37	0.58	0.37	0.23	0.29
5 3 4 5 5	0.26	0.11	0.24	0.33	0.17	0.28	0.32	0.23	0.23
5 3 5 5 5	0.26	0.12	0.23	0.33	0.20	0.26	0.34	0.22	0.26
5 4 4 5 5	0.31	0.12	0.30	0.54	0.32	0.43	0.34	0.23	0.24
5 4 5 5 5	0.32	0.12	0.29	0.66	0.32	0.59	0.37	0.23	0.28
5 5 4 5 5	0.23	0.11	0.21	0.63	0.36	0.49	0.33	0.23	0.24
5 5 5 5 5	0.24	0.12	0.21	0.64	0.36	0.53	0.36	0.23	0.29

* – G+C dev. means that both transconductors and capacitors were deviated, G dev. (resp. C dev.) refers to the situation when only transconductors (respectively: capacitors) were deviated.

Table 2

Maximum deviation of amplitude for 5-th order all-pole low-pass Butterworth filters*

Odchylenie maksymalne amplitudy dla dolnoprzepustowych filtrów Butterwortha 5-go rzędu

Filter structure	ω=0.5			ω=1.0			ω=2.0		
	G+C dev.	C dev.	G dev.	G+C dev.	C dev.	G dev.	G+C dev.	C dev.	G dev.
2 3 4 5 5	0.36	0.08	0.35	0.56	0.29	0.42	0.70	0.39	0.45
2 3 5 5 5	0.37	0.09	0.35	0.61	0.31	0.45	0.75	0.40	0.48
2 4 4 5 5	0.36	0.09	0.32	0.81	0.46	0.59	0.65	0.40	0.48
2 4 5 5 5	0.38	0.09	0.35	0.96	0.47	0.77	0.68	0.43	0.51
2 5 4 5 5	0.30	0.09	0.24	0.97	0.52	0.67	0.67	0.37	0.47
2 5 5 5 5	0.29	0.09	0.25	0.94	0.53	0.81	0.71	0.39	0.52
3 3 4 5 5	0.46	0.16	0.33	0.76	0.42	0.62	0.84	0.42	0.46
3 3 5 5 5	0.43	0.17	0.41	0.88	0.41	0.62	0.74	0.42	0.46
3 4 4 5 5	0.64	0.17	0.52	0.16	0.62	0.83	0.76	0.41	0.46
3 4 5 5 5	0.61	0.19	0.54	1.35	0.60	1.11	0.73	0.44	0.52
3 5 4 5 5	0.37	0.17	0.35	1.19	0.58	0.89	0.68	0.40	0.50
3 5 5 5 5	0.48	0.17	0.34	1.31	0.61	1.00	0.76	0.42	0.57
4 3 4 5 5	0.46	0.15	0.44	0.67	0.29	0.51	0.70	0.39	0.45
4 3 5 5 5	0.53	0.17	0.40	0.79	0.38	0.66	0.74	0.39	0.46
4 4 4 5 5	0.54	0.16	0.50	1.12	0.55	0.93	0.68	0.43	0.45
4 4 5 5 5	0.60	0.19	0.52	1.54	0.57	1.27	0.83	0.40	0.59
4 5 4 5 5	0.41	0.15	0.35	1.21	0.58	0.95	0.68	0.40	0.46
4 5 5 5 5	0.43	0.19	0.36	1.40	0.60	1.20	0.75	0.39	0.57
5 3 4 5 5	0.61	0.18	0.44	0.67	0.26	0.53	0.65	0.41	0.44
5 3 5 5 5	0.53	0.18	0.44	0.65	0.32	0.51	0.66	0.42	0.56
5 4 4 5 5	0.60	0.17	0.58	1.14	0.59	0.76	0.65	0.40	0.54
5 4 5 5 5	0.68	0.19	0.62	1.42	0.50	1.22	0.72	0.42	0.60
5 5 4 5 5	0.51	0.17	0.38	1.27	0.57	0.93	0.63	0.42	0.48
5 5 5 5 5	0.53	0.19	0.39	1.32	0.60	1.12	0.76	0.40	0.52

* – G+C dev. means that both transconductors and capacitors were deviated, G dev. (resp. C dev.) refers to the situation when only transconductors (respectively: capacitors) were deviated.

To simplify further description, we introduce the following notation: let the sequence $j_1,j_2,...,j_n$ denote the canonical all-pole low-pass structure of n-th order, for which the feedback signal emerging at node x_i is taken from node x_{j_i}. For example, n-th order LF structure will be denoted as 2,3,4,...,n,n, while n-th order IFLF structure as n,n,...,n.

Here, we consider 5-th order Butterworth filters. According to the discussion above, there are 24 different canonical structures that realize this transfer function. They can be implemented with the same value of transconductances for all filter transconductors (see [23] for more details). Table 1 and 2 show the standard and maximum deviation of amplitude, respectively, for all considered filter structures, obtained for 5000 random samples. 1% deviation in capacitance elements, transconductance elements or all filter elements has been assumed (with gaussian distribution for standard deviation and with flat distribution for maximum deviation). The simulations have been performed for normalised frequency equal to 0.5, 1.0 and 2.0. It follows that for low frequency (ω=0.5) transconductance element deviations determine the deviation of transfer function of the filter. For higher frequencies (ω=2.0) the contributions of transconductance and capacitance element deviations becomes roughly the same. It is also seen that transfer function deviation is larger for IFLF filter than for LF one. Note that there is a kind of monotonic dependence between the filter structure and transfer function deviation. In particular, the more the filter is similar to LF one, the smaller transfer function deviation it exhibits. The similarity is 'measured' by the number of feedback transconductors located in the same place as in LF filter (see also [25] for more detailed discussion on this subject).

5. CONCLUSIONS

In the paper, an efficient procedure for calculating deviation of filter transfer function given deviations of filter element values has been developed. The procedure has been used to perform statistical analysis of G_m-C filters. It follows that accuracy of the results obtained by means of the method is very good, provided that the deviations of filter element values are not larger than 5–10% (depending on the considered filter). A number of examples that illustrate the proposed approach have been presented including statistical analysis of family of filters realizing the same all-pole low-pass transfer function of 5^{th} order. The computational complexity of the proposed procedure is $O(n^2)$, while the complexity of the exact method is $O(n^3)$ since it involves inverting n(n matrix during each iteration. It is also worth noticing that the proposed method is versatile, since it can be applied to any G_m-C filter structure using the same general formulas (and, as a consequence, the same software packages).

6. ACKNOWLEDGEMENT

The author would like to thank the anonymous reviewer for his comments and remarks which were helpful in improving the quality of the paper.

7. REFERENCES

1. R. Schaumann, M.S. Ghausi, K.R. Laker: *Design of Analog Filters, Passive, Active RC, and Switched Capacitor*. Englewood Cliff, NJ: Prentice-Hall, 1990.

2. T. Deliyannis, Y. Sun, J.K. Fidler: *Continuous-time active filter design*. CRC Press, USA, 1999.
3. C. Toumazou, J. Lidgey, D. Haigh, Eds.: *Analogue IC Design – The Current-Mode Approach*. London, U.K.: IEE, Apr. 1990.
4. R.L. Geiger, E. Sánchez-Sinencio: *Active filter design using operational transconductance amplifiers: A tutorial*. IEEE Circuit and Devices Mag., March 1985, vol. 1, pp. 20–32.
5. E. Sánchez-Sinencio, R.L. Geiger, H. Nevarez-Lozano: *Generation of Continuous-Time Two Integrator Loop OTA Filter Structures*. IEEE Trans. Circuits Syst., August 1988, vol. 35, pp. 936–946.
6. M.A. Tan, R. Schaumann: *Design of a General Biquadratic Filter Section with Only Transconductances and Grounded Capacitors*. IEEE Trans. Circuits Syst.-II, April 1988, vol. 35, pp. 478–480.
7. G. Groenewold: *Optimal Dynamic Range Integrated Continuous-Time Filters*. Delft, The Netherlands: Delft Univ. Press, 1992.
8. G. Groenewold: *The Design of High Dynamic Range Continuous-Time Integratable Bandpass Filters*. IEEE Trans. Circuits and Syst., August 1991, vol. 38, No.8, pp. 838–852.
9. B. Nauta: *Analog CMOS filters for very high frequencies*. Kluwer Academic Publishers, 1993.
10. J. Silva-Martinez, M.S.J. Steyaert, W. Sansen: *A 10.7MHz 68-dB CMOS continuous-time filter with on-chip automating tuning*. IEEE J. Solid-State Circuits, 1992, vol. 27, No. 12, pp. 1843–1853.
11. R. Allini, A. Baschirotto, R. Castello: *Tuneable BiCMOS continuous-time filter for high-frequency applications*. IEEE J. Solid-State Circuits, 1992, vol. 27(12), pp.1905–1915.
12. Y.P. Tsividis: *Integrated continuous-time filter design – An overview*. IEEE J. Solid-State Circuits, March 1994, vol. 29, pp. 166–176.
13. S. Szczepański, J. Jakusz, R. Schaumann: *A linear CMOS OTA for VHF applications*. IEEE Trans. Circuits Syst.-II, March 1997, vol.44, pp. 174–187.
14. J. Mahattanakul, C. Toumazou: *Current-Mode Versus Voltage-Mode G_m-C Biquad Filters: What the Theory Says*. IEEE Trans. Circuits Syst.-II, February 1998, vol. 45, pp. 173–186.
15. J. Glinianowicz, J. Jakusz, S. Szczepański, Y. Sun: *High-frequency two-input CMOS OTA for continuous-time filter applications*. IEE Proc.-Circuits Dev. Syst., February 2000, vol.147, No.1, pp.13–18.
16. M.S. Ghausi, K.R. Laker: *Modern Filter Design: Active RC and Switched Capacitor*. Englewood Cliffs, NJ, Prentice-Hall, Inc., 1981.
17. G.W. Roberts, A.S. Sedra: *A general class of current amplifier-based biquadratic filter circuits*. IEEE Trans. Circuits Syst.-I, April 1992, vol. 38, pp. 257–263.
18. G.W. Roberts, A.S. Sedra: *All current-mode frequency selective circuits*. Electron. Lett., June 1989, vol. 25, pp. 759–761.
19. J.D. Schoeffler: *The synthesis of minimum sensitivity networks*. IEEE Trans. Circuit Theory, 1964, vol. 11, pp. 271–276.
20. R. Mackay, A.S. Sedra: *Generation of low-sensitivity state-space active filters*. IEEE Trans. Circuit Syst., October 1980, vol. CAS-27, pp. 863–870.
21. S. Kozieł, S. Szczepański: *Dynamic Range Comparison of Voltage-Mode and Current-Mode State-Space G_m-C Biquad Filters in Reciprocal Structures*. Proc. IEEE Int. Conf. Elect. Circuits Syst., 2001, vol. II, pp. 819–822.
22. S. Kozieł, S. Szczepański, R. Schaumann: *General Approach to Continuous-Time G_m-C Filters Based on Matrix Description*. Proc. Int. Symp. Circuits, Syst., ISCAS, Phoenix, AZ, USA, 2002, vol.IV, pp. 647–650.
23. S. Kozieł, S. Szczepański, R. Schaumann: *General Approach to Continuous-Time G_m-C Filters*. To appear, 2003, Int. J. Circuit Theory and Applications.
24. S. Kozieł, S. Szczepański: *Structure Generation and Performance Comparison of Canonical Elliptic G_m-C Filters*. Proc. Int. Conf. Electron. Circuits, Syst., ICECS, vol. I, pp. 157–160, Dubrovnik, Croatia, 2002.
25. S. Kozieł, S. Szczepański: *Sensitivity Properties of All-Pole Canonical Low-Pass G_m-C Filters*. Proc. IEEE Int. Conf. Circuits Syst. for Communications, ICCSC'2002, St. Petersburg, Russia, 2002, pp. 54–57.

S. KOZIEŁ

EFEKTYWNA ANALIZA TOLERANCJI FILTRÓWAKTYWNYCH G_m-C CZASU CIĄGŁEGO

Streszczenie

W pracy przedstawiono efektywną metodę analizy tolerancji dla filtrów aktywnych G_m-C czasu ciągłego. Zaprezentowano ogólny opis macierzowy filtrów G_m-C, który obejmuje wszystkie możliwe realizacje filtrów w rozważanej klasie elementów. Zaletą tego opisu jest między innymi to, że wszystkie macierze występujące w równaniach mogą być tworzone bezpośrednio przez wgląd w schemat układu.

W oparciu o przedstawiony model wyprowadzono formuły umożliwiające wyznaczanie tolerancji funkcji przenoszenia filtru (zarówno modułu jak i fazy) przy zadanych odchyłkach wartości elementów filtru od wartości nominalnych. Zastosowano pewne przybliżenie, które przy założeniu małych odchyłek wartości elementów filtru umożliwia obliczanie odchyłki funkcji przenoszenia bez konieczności odwracania macierzy głównej układu równań opisujących filtr przy każdorazowej zmianie wartości odchyłek elementów. Powoduje to zmniejszenie asymptotycznej złożoności obliczeniowej całej procedury z $O(n^3)$ do $O(n^2)$.

Przedstawioną metodę wykorzystano do przeprowadzenia analizy statystycznej filtrów G_m-C. W szczególności, dokonano analizy Monte Carlo i analizy najgorszego przypadku (Worst Case) dla wybranych struktur filtrów różnych rzędów. Zaprezentowano również wyniki analizy porównawczej rodziny filtrów realizujących tą samą dolnoprzepustową funkcję przenoszenia piątego rzędu.

Przedstawione wyniki eksperymentów pokazują, że wzory przybliżone dają bardzo dobre rezultaty przy odchyłkach wartości elementów układu nie przekraczających 5–10% od wartości nominalnej w zależności od badanej struktury filtru, przy czym uzyskano kilkukrotne zmniejszenie czasu obliczeń (w porównaniu do metody dokładnej) już dla filtrów o średniej złożoności (6–8 rzędu). Należy również zaznaczyć, że opisana procedura jest uniwersalna i pozwala analizować dowolne struktury filtrów G_m-C za pomocą tego samego programu komputerowego. Może ona zatem być wykorzystana w systemach automatycznego projektowania i analizy filtrów tej klasy.

Słowa kluczowe: filtry G_m-C, analiza tolerancji, analiza statystyczna